A Novel Technique for Detecting Electromagnetic Wave Caused by Partial Discharge in GIS

Toshihiro Hoshino, Katsumi Kato, Naoki Hayakawa, *Member, IEEE*, and Hitoshi Okubo, *Member, IEEE*

***Abstract*—For the insulation diagnosis of GIS, it is necessary to detect partial discharge (PD) under noisy condition and to specify the direction of electromagnetic wave radiation due to PD. We proposed "phase gate control method" for discriminating the electromagnetic wave caused by PD in SF_6 gas from external noises. The proposed method enabled us to discriminate PD of about 100 pC in SF_6 gas from external noises of more than 10 000 pC in air. We also compared polarization characteristics of electromagnetic wave radiated from PD with those from a half-wave dipole antenna, and could estimate the radiation length of electromagnetic wave caused by PD. The results derived in this paper will make a great contribution to the insulation diagnosis of GIS on-site.**

***Index Terms*—Electromagnetic wave spectrum, gas insulated switchgear, noise elimination, partial discharge, polarization.**

I. Introduction

IN ORDER to supply electric power with high reliability, the insulation diagnosis of high voltage power apparatus like SF_6 gas insulated switchgears (GIS) is needed. The partial discharge (PD) measurement is a promising technique to prevent the breakdown in GIS and to keep the high performance of electrical insulation. Many researches related to the diagnosis technique for GIS have been reported [1]–[5], and various kinds of PD sensors, especially UHF sensors [6]–[9], have been developed.

However, there exist external noises inside and outside GIS on-site [10], [11]. Therefore, an advanced technique is indispensable to discriminate small PD signal in SF_6 gas from large external noises [12]–[14] and to improve the sensitivity for detecting harmful PD signal in GIS. Furthermore, for the open-air substations, it is very difficult to identify the location of the electromagnetic wave radiation due to PD, because many electromagnetic apertures like bushings, bus-bars, transmission lines would become radiation sources of electromagnetic wave. Therefore, the identification technique of electromagnetic wave caused by PD is required to be developed.

We have been investigating the detection technique of electromagnetic wave caused by PD for the insulation diagnosis of GIS on-site [15], [16]. In this paper, we propose "phase gate control method" to separate the electromagnetic wave caused by PD in SF_6 gas from external noises in air. We also focus on the polarization characteristics of electromagnetic wave radiated from PD, and point out that they are quite similar to those from a half-wave dipole antenna. The results help us to identify the radiation length of electromagnetic wave due to PD.

Manuscript received March 23, 1999.

The authors are with the Department of Electrical Engineering, Nagoya University, Nagoya, Japan.

Publisher Item Identifier S 0885-8977(01)08516-8.

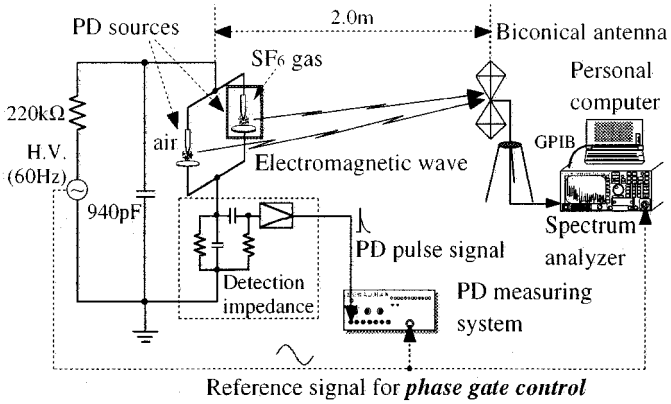

Fig. 1. Experimental setup for measuring electromagnetic wave radiated from PD.

II. Discrimination of PD Signal in SF_6 Gas Using Phase Gate Control Method

In this chapter, a novel technique is introduced for the discrimination of the electromagnetic wave due to PD from external noises.

A. Experimental Setup

Fig. 1 shows the experimental setup for measuring electromagnetic wave caused by PD. The PD was generated by simultaneously applying ac high voltage to needle-plane electrodes with the gap length of 15 mm in both air and SF_6 gas. The electromagnetic wave radiated from the PD was received by a biconical antenna (30∼300 MHz) or a log-periodic antenna (80 MHz∼1 GHz). Each antenna was located at the distance of 2 m from the PD source, and was set vertically to the ground. The output signal of the antenna was transferred into a spectrum analyzer in such a way that the maximum electric field strength in each frequency was held for 30 s.

Fig. 2(a) and (b) shows typical relationship between PD charge and voltage phase angle in air and SF_6 gas, respectively. The PD pulse signals were detected by detection impedance in Fig. 1, and were phase-resolved in the applied ac voltage by using the reference signal. Note that the positive PD charges in air are extremely large in comparison with those in SF_6 gas. From the result, PD pulse mechanism in ac positive half cycles is greatly different from that in negative half cycles, and thus the electromagnetic wave due to the positive and the negative

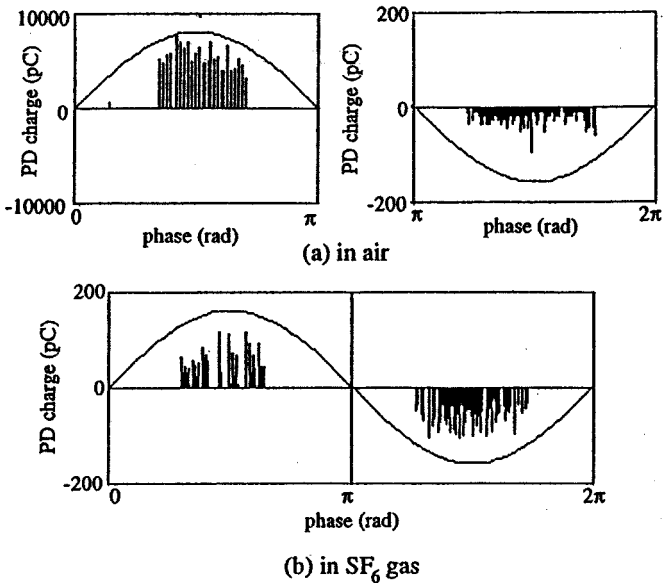

Fig. 2. Phase-resolved PD pulses in air and SF_6 gas.

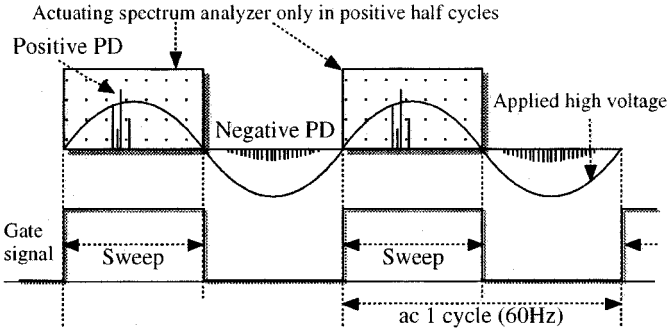

Fig. 3. Phase gate control method. (Gate signal is applied to ac positive half cycles.)

PD also differs. Therefore, separate measurement of these electromagnetic waves can be expected to discriminate the PD signals from external noises.

In order to focus on the specific PD signals and the corresponding electromagnetic wave occurring in different phases of the applied ac voltage, we divided an ac cycle of the applied ac voltage into positive and negative half cycles as shown in Fig. 3. We call the measuring method as "phase gate control method." The gate signal in Fig. 3 is made from the ac reference signal in Fig. 1 and can be controlled to an arbitrary phase width. Thus, we can measure the electromagnetic wave occurring in the designated phase region of applied voltage.

B. Discrimination of PD in SF_6 Gas From External Noises

Fig. 4 shows the frequency spectrum of electromagnetic wave caused by PD's in both SF_6 gas and air. This spectrum was received by the biconical antenna for the applied voltage $V_{ac} = 10.5\ \mathrm{kV_{rms}}$ without the phase gate control. Solid and broken lines in Fig. 4 represent the spectrum of PD and back ground noise (BGN), respectively. The BGN spectrum consists of various broadcasting waves such as at 80, 180, 200, 250 and 280 MHz. The spectrum caused by both PD in SF_6 gas and air

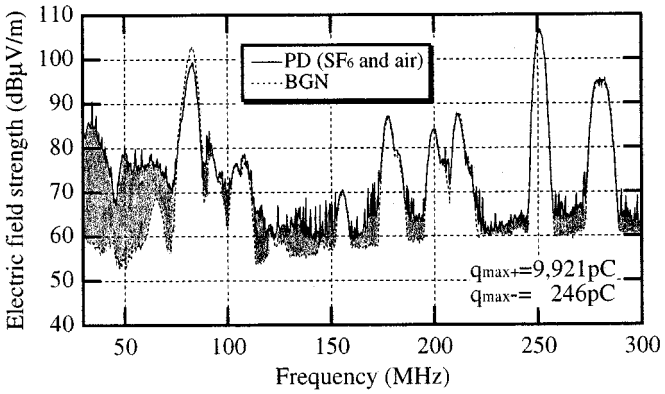

Fig. 4. Electromagnetic wave spectrum caused by both PD in SF_6 gas and air. (No application of phase gate control method.)

is observed as the difference between solid and broken lines. The gain of PD spectrum is 5∼25 dB in the frequency ranges from 30 to 300 MHz. Note that the maximum PD charge in positive half cycles in air is 9921 pC, which is about 40 times larger than that in negative half cycles. Therefore, the influence of the external noises due to positive PD in air is remarkable.

Here, we try to remove the spectrum due to the positive PD pulses by using the phase gate control method. Fig. 5 shows the electromagnetic wave spectra in ac negative half cycles with the phase gate control, where PD's occur in (a) both SF_6 gas and air, (b) air alone, and (c) SF_6 gas alone, respectively. In Fig. 5(a), the pulsive spectrum as was shown in Fig. 4 is eliminated, and the gains at (1)∼(3) are smaller than those in Fig. 4. Therefore, the gain in Fig. 4 mainly arises from the positive PD pulses in air with the maximum charge of about 10 000 pC. On the other hand, the gain of negative PD in air in Fig. 5(b) appears only in the frequency range from 30 to 75 MHz marked with (4). However, the gain in SF_6 gas in Fig. 5(c) emerges in the frequency ranges marked with (5)∼(7). Therefore, the gains marked with (2) and (3) in Fig. 5(a) can be seen to arise from negative PD pulses in SF_6 gas. From these results, the phase gate control method enables us to discriminate small spectrum gain in SF_6 gas, which improves the sensitivity of PD detection.

The phase gate control method is also available to discriminate the PD spectrum in SF_6 gas in UHF band as well as that in VHF band. Fig. 6 shows the electromagnetic wave spectrum in ac negative half cycles, where PD's occur in (a) both SF_6 gas and air, (b) air alone, and (c) SF_6 gas alone, respectively. The spectra in Fig. 6 were received by a log-periodic antenna in the frequency range from 80 MHz to 1000 MHz. The maximum charge of positive PD in air was 14 000 pC, while that of negative PD in air and SF_6 gas was 242 pC and 190 pC, respectively. The PD spectrum marked with (1)∼(3) is detected in Fig. 6(a), while PD spectrum in air alone is not found as shown in Fig. 6(b). However, PD spectrum in SF_6 gas alone marked with (4)∼(6) in Fig. 6(c) appear in the same frequency ranges as that in Fig. 6(a). Therefore, the gains marked with (1)∼(3) in Fig. 6(a) arise from negative PD pulses in SF_6 gas.

The above experimental results indicate that selecting phase regions of the applied ac voltage permits to detect PD signals as small as 100 pC in SF_6 gas under external noises with 10 000 pC in air. Therefore, the phase gate control method can be expected

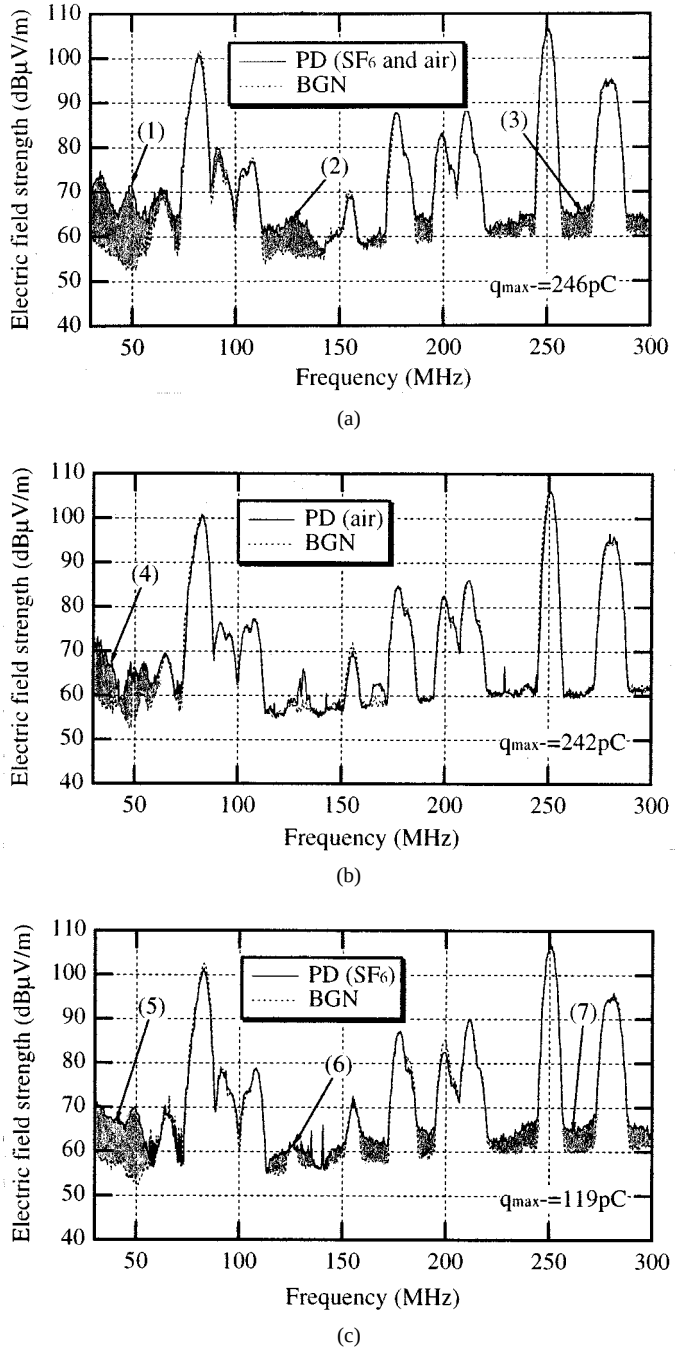

Fig. 5. Electromagnetic wave spectra by negative PD received by biconical antenna. (Phase gate control method is applied to ac negative half cycles.) (a) PD in both SF_6 gas and air. (b) PD in air alone. (c) PD in SF_6 gas alone.

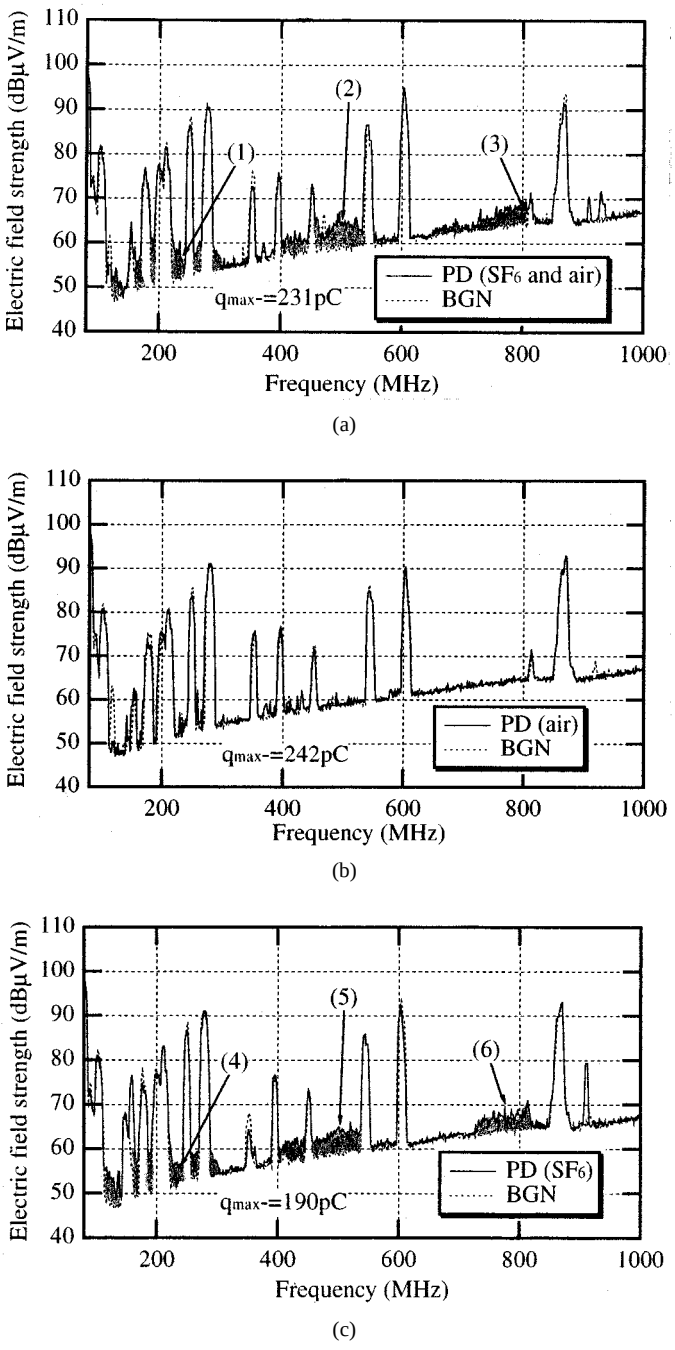

Fig. 6. Electromagnetic wave spectra by negative PD received by log-periodic antenna. (Phase gate control method is applied to ac negative half cycles.) (a) PD in both SF_6 gas and air. (b) PD in air alone. (c) PD in SF_6 gas alone.

to be a high-sensitive technique for discriminating PD signals in SF_6 gas even under noisy conditions.

C. Delectable Frequency Zone of PD Signal in SF_6 Gas

In the same way as that in the previous section, we can investigate the detectable frequency zone of PD signal in SF_6 gas. Fig. 7 shows the PD-detectable zone where PD in SF_6 gas as alone can be discriminated from that in air for (a) positive and (b) negative half cycles. Symbols • and × denote the maximum PD charge at the corresponding frequencies. The shadow region between noise mixed zone and undetected zone means the PD-detectable zone in SF_6 gas. With increasing the frequency, the upper boundary becomes sharp, while the lower boundary is smooth. The result can be interpreted in terms of the difference in the frequency component of PD pulses in SF_6 gas and in air; PD pulses in SF_6 gas have higher frequency components than those in air [3]. Therefore, the spectrum of PD in SF_6 gas remains in higher frequency range.

From these results, S/N ratio can be improved to detect small PD signals in SF_6 gas by selecting higher frequency range together with the phase gate control method.

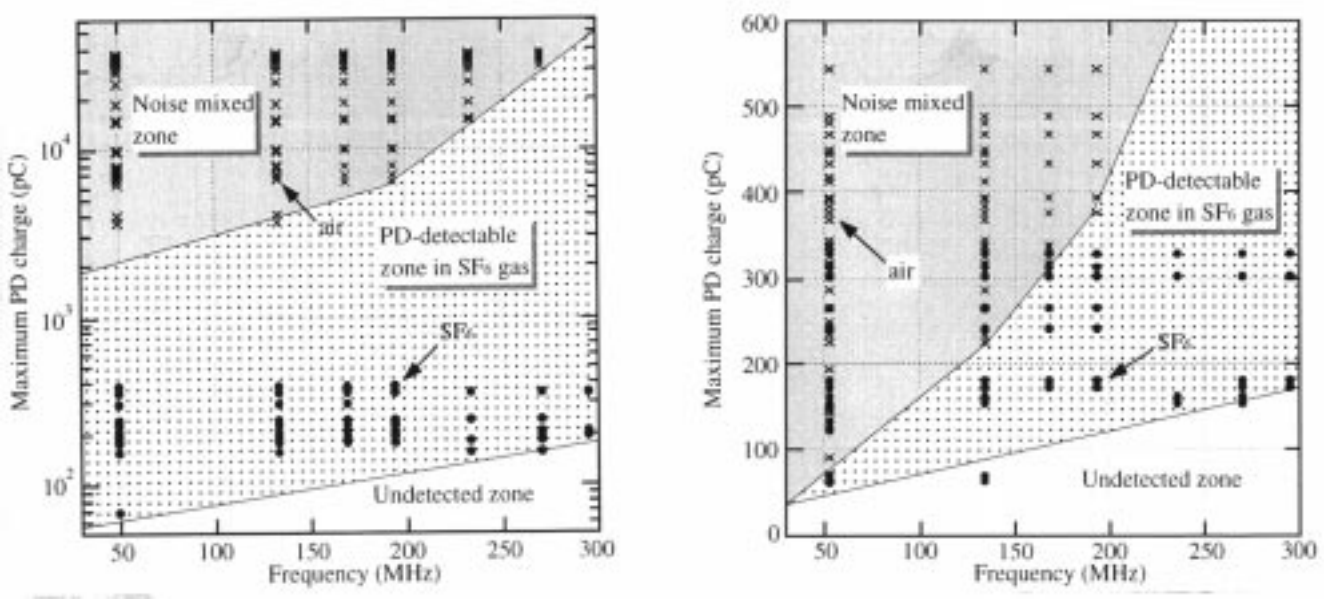

Fig. 7. PD-detectable zone in SF_6 gas under noisy condition. (a) Positive half cycles. (b) Negative half cycles.

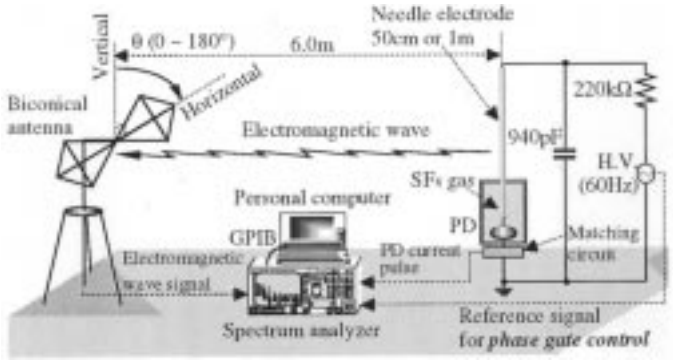

Fig. 8. Experimental setup for measuring polarization angle of electromagnetic wave radiated from PD.

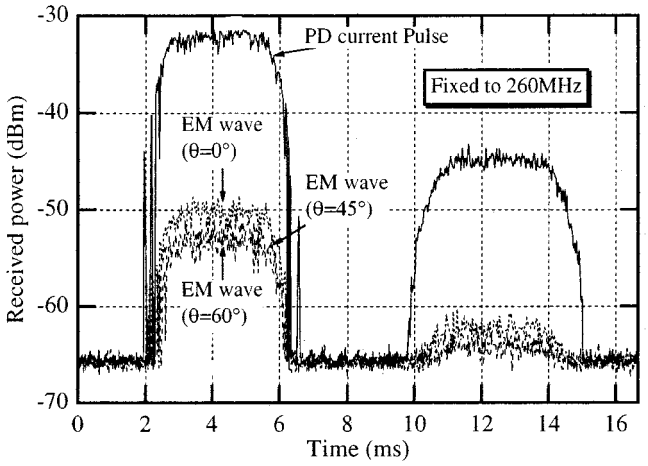

Fig. 9. Time-resolved spectra of both PD current pulse and electromagnetic waves in ac 1 cycle fixed to 260 MHz.

III. Identification of Radiation Length Based on Polarization Characteristics

In order to locate the PD source, we developed in this chapter the identification technique of radiation length of electromagnetic wave caused by PD.

A. Experimental Setup

Fig. 8 shows the experimental setup for measuring polarization angle of electromagnetic wave caused by PD. The PD with the charge of about 500∼600 pC was generated by applying 14.0 kV_{rms} to the needle-plane electrode in SF_6 gas at 0.1 MPa. The electromagnetic wave radiated from the PD was received by the biconical antenna which was set 6 m apart from the PD source. Moreover, we replaced the PD source with dipole antennas to compare the polarization characteristics of electromagnetic wave. Two half-wave dipole antennas with the length of 50 cm and 1 m, and an infinitesimal dipole antenna with the length of 3 cm were used for the calibration. The element of the biconical antenna was rotated for the adjustment to the polarization angle θ (0∼180°) as shown in Fig. 8.

The received electromagnetic wave at each polarization angle θ was transferred into the spectrum analyzer. PD current pulses were also measured with the spectrum analyzer through a matching circuit with the frequency response of higher than 1 GHz. In the measurement, the phase gate control method enables us to compare the phase-resolved spectrum of PD current pulse with that of the corresponding electromagnetic wave in an ac cycle of the applied voltage.

B. Polarization Angle θ_{min} With Minimum Received Power

The received spectrum of electromagnetic wave varies with the rotation angle θ of the biconical antenna. Fig. 9 shows the typical received spectra of both PD current pulse and the corresponding electromagnetic waves for $\theta = 0°$, 45°, 60°. These spectra are time-resolved in ac 1 cycle fixed to 260 MHz as an example. The received spectra appear in both positive and negative peak phases and the electromagnetic wave spectra depend

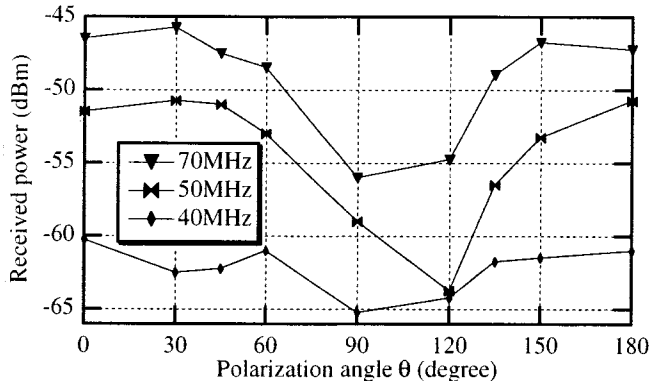

Fig. 10. Relation between received power and polarization angle as a parameter of frequency.

on the rotating angle θ. This result means that there exists the polarization of electromagnetic wave due to PD.

Fig. 10 shows the received power in the positive peak phase for $0° \leq \theta \leq 180°$. The received power takes the minimum value at $\theta_{\min} = 90°$ in 40 MHz and 70 MHz, while at $\theta_{\min} = 120°$ in 50 MHz. The result indicates that the polarization angle θ for the minimum received power depends on the frequency.

C. Polarization Characteristics of Half-Wave Dipole Antenna and Infinitesimal Dipole Antenna

The polarization angle $\theta_{\min}$ is calibrated by using dipole antennas with the known radiation length. The results are shown in Fig. 11. When the half-wave dipole antenna with the length of 1 m was set vertically ($\triangle$) to the ground in Fig. 11(a), $\theta_{\min}$ is verified to be about 90° in (the whole frequency range. On the other hand, when the dipole antenna was set horizontally ($\bullet$), $\theta_{\min}$ becomes about 0° beyond 110 MHz. Thus, the polarization angle beyond 110 MHz coincides well with the theoretical value of the half-wave dipole antenna. Next, the calibration result is obtained in Fig. 11(b) for the half-wave dipole antenna with the length of 50 cm. The critical frequency range where $\theta_{\min}$ becomes 0° for the horizontal dipole arrangement or 90° for the vertical dipole arrangement is beyond 190 MHz, which is higher than 110 MHz in Fig. 11(a). This may be attributed to that the resonance frequency f_r of the half-wave dipole antenna increases from 150 MHz to 300 MHz as will be mentioned later. However, for the infinitesimal dipole antenna with the length of 3 cm in Fig. 11(c), the polarization angle becomes irrespective of the arrangement of the dipole element, as was shown below 70 MHz in Fig. 11(a), and below 140 MHz in Fig. 11(b).

Based on the above results, we can classify the frequency range for the polarization angle of dipole antennas into 3 groups as shown in Table I, together with the measurement results in Fig. 11. The 3 frequency ranges strongly depend on f_r; in the frequency range lower than $f_r/2$, $\theta_{\min}$ has no relation with the rotation angle of the dipole element. On the other hand, in the frequency range higher than $2f_r/3$, $\theta_{\min}$ becomes perpendicular to the element of the dipole antenna. These results mean that a dipole antenna could behave as the infinitesimal dipole antenna in the lower frequency range than $f_r/2$, while as the half-wave dipole antenna in the higher frequency range than $2f_r$ / 3. The

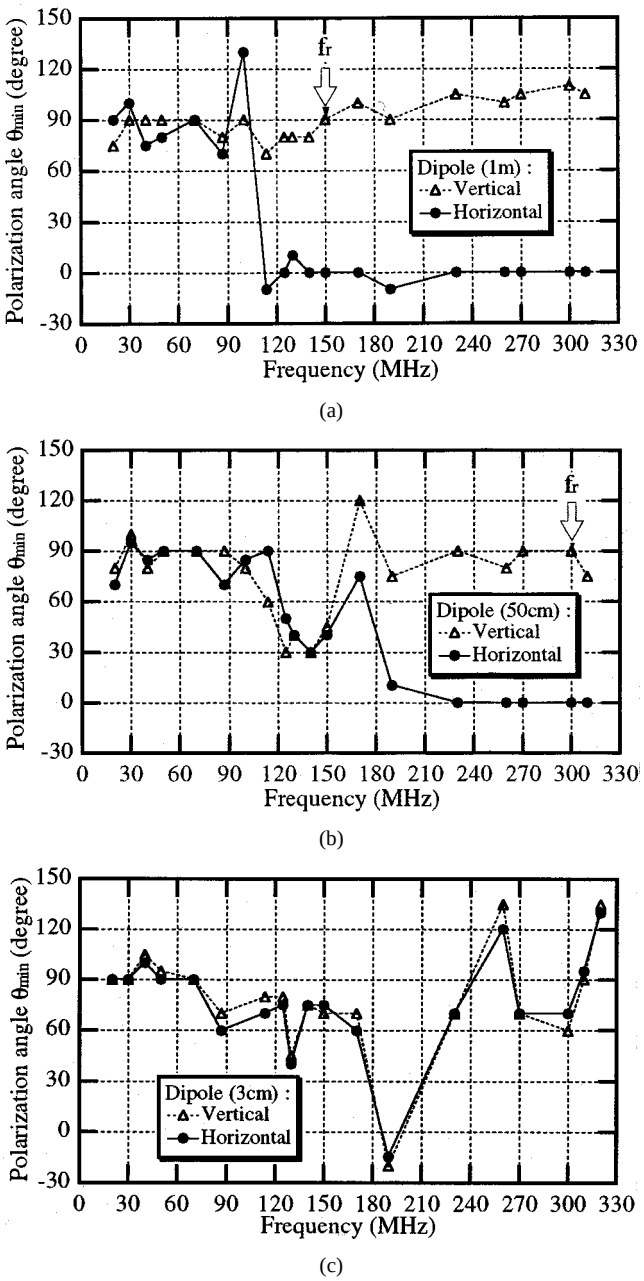

Fig. 11. Relation between polarization angle and frequency for different dipole antennas. (a) 1 m half-wave dipole antenna (fr = 150 MHz). (b) 50 cm half-wave dipole antenna (fr = 300 MHz). (c) 3 cm infinitesimal dipole antenna (fr = 5 GHz).

3 frequency ranges shift to the lower frequency side as the longer radiation length of the dipole antenna.

D. Polarization Characteristics of PD Signal and Specification of Radiation Length of PD Source

In this section, we investigate the polarization characteristics of the electromagnetic wave caused by PD and compare them with those of the dipole antenna in the previous section. Fig. 12 shows the polarization angle $\theta_{\min}$ for PD with various needle lengths. The needle-plane electrode in Fig. 8 was set vertically or horizontally to the ground instead of half-wave and infinitesimal dipole antennas.

TABLE I
CLASSIFICATION OF FREQUENCY RANGE FOR ELECTROMAGNETIC WAVE DUE TO DIPOLE ANTENNAS

	Infinitesimal dipole $f \leqq f_r/2$	Transient range $f_r/2 \leqq f \leqq 2f_r/3$	Half-wave dipole $2f_r/3 \leqq f$
2L = 1m f_r=150MHz	≦75MHz (70MHz)	75~100MHz (70~110MHz)	100MHz≦ (110MHz)
2L = 50cm f_r=300MHz	≦150MHz (140MHz)	150~200MHz (140~190MHz)	200MHz≦ (190MHz)
2L = 3cm f_r=5GHz	≦2.5GHz	2.5~3.3GHz	3.3GHz≦

L: half length of dipole antenna.
Measurement results in Fig.11 are in parentheses.

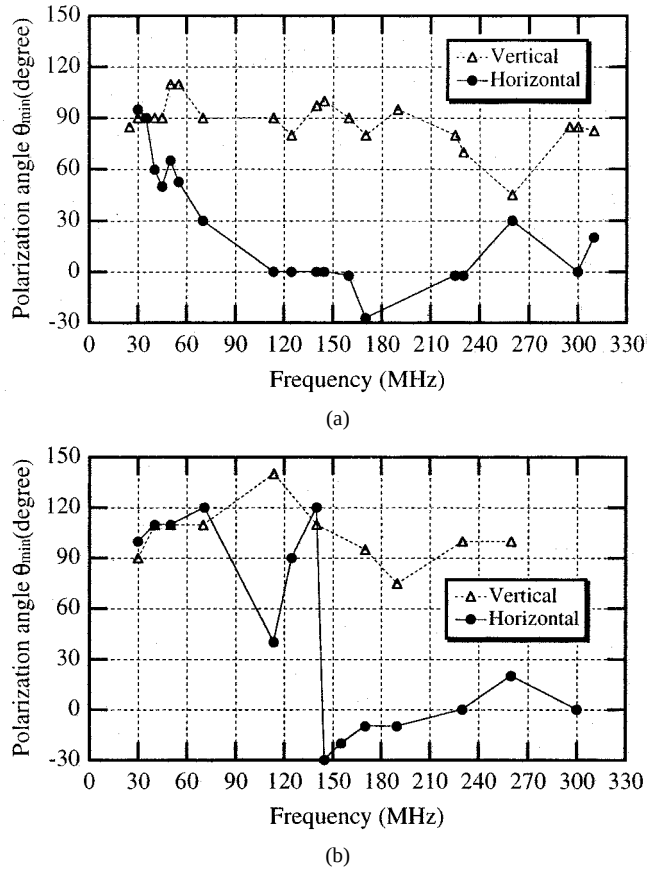

Fig. 12. Polarization characteristics of electromagnetic wave due to PD. (a) Needle electrode: 1 m. (b) Needle electrode: 50 cm.

In Fig. 12(a) for the needle length of 1 m, the polarization characteristic beyond 110 MHz corresponds to that of the 1 m half-wave dipole antenna in Fig. 11(a). The critical frequency in Fig. 12(b) is obtained as 170 MHz for the needle length of 50 cm. In the same way, the polarization characteristic below 30 MHz in Fig. 12(a) corresponds to that of the 1 m half-wave dipole antenna in Fig. 11(a). The critical frequency in Fig. 12(b) is obtained as 70 MHz for the needle length of 50 cm. The classification of frequency range for electromagnetic wave due to PD is shown in Table II. The polarization characteristic of the electromagnetic wave radiated from PD coincides well with that from half-wave dipole antenna with the same radiation length.

TABLE II
CLASSIFICATION OF FREQUENCY RANGE FOR ELECTROMAGNETIC WAVE DUE TO PD

	Infinitesimal dipole	Transient range	Half-wave dipole
2L=1m	≦30MHz	30~110MHz	110MHz≦
2L = 50cm	≦70MHz	70~170MHz	170MHz≦

Therefore, the measurement of polarization characteristic of PD enables us to specify the radiation length of electromagnetic wave caused by PD. The specification of the radiation length can be applied to the identification of radiation source of electromagnetic wave like spacer apertures, bushings, bus-bars, transmission lines and so on. Consequently, the polarization characteristics can be utilized to identify the PD source in GIS on-site. Moreover, by rotating the polarization angle of PD-detecting antenna on the basis of polarization characteristics, the detection sensitivity of electromagnetic wave due to PD can he enhanced.

IV. CONCLUSION

We developed the advanced detection technique of electromagnetic wave caused by PD in GIS. At first, we proposed the "phase control method" to discriminate PD signals in SF_6 gas from external noises in air. PD signals of 100 pC in SF_6 gas could be successfully discriminated from external noises of 10 000 pC in air. We also clarified the PD-detectable area where the PD signals in SF_6 gas would he detected under noisy conditions. Experimental results revealed that the S/N ratio to detect small PD signals in SF_6 gas was improved by selecting higher frequency range together with the phase gate control method.

Furthermore, we investigated the polarization angle $\theta_{\min}$ with the minimum received power of the electromagnetic wave at different frequencies, and compared the polarization characteristics between PD and the dipole antennas with different radiation lengths. Experimental results revealed that the polarization characteristic of PD for needle-plane electrode corresponded to those for half-wave dipole antennas with the same length. Therefore, the polarization characteristic of PD enabled us to specify the radiation length of electromagnetic wave due to PD. The results derived in this paper will make a great contribution to the electrical insulation diagnosis of GIS on-site.

REFERENCES

[1] F. Endo, *et al.*, "Insulation diagnostic system of GIS," in *8th International Symposium on High Voltage Engineering*, vol. 3, 1993, no. 66.01, pp. 145–148.
[2] M. Visintin, *et al.*, "The characteristics of partial discharge from particles in GIS," in *IEEE International Symposium on Electrical Insulation*, 1994, pp. 277–282.
[3] M. Hikita, *et al.*, "Phase dependence of partial discharge current pulse waveform and its frequency characteristics in SF_6 gas," in *IEEE International Symposium on Electrical Insulation*, vol. 1, 1996, pp. 103–106.
[4] T. Sakakibara, *et al.*, "Study of propagation phenomena of partial discharge pulses in gas insulated substation," *IEEE Trans. Power Delivery*, vol. 13, no. 3, pp. 768–776, 1998.
[5] E. Gulski, "Computer-aided measurement of partial discharge in HV equipment," *IEEE Trans. Electrical Insulation*, vol. 28, no. 6, pp. 969–983, 1993.

[6] A. Petit, "Field experience of partial discharge monitoring with the UHF method," in *9th International Symposium on High Voltage Engineering*, 1995, no. 5596.
[7] M. D. Judd, *et al.*, "Partial discharge excitation of UHF modes in a cylindrical cavity," in *9th International Symposium on High Voltage Engineering*, 1995, no. 4561.
[8] R. Kurrer, *et al.*, "The application of ultra-high-frequency partial discharge measurements to gas-insulated substations," *IEEE Trans. Power Delivery*, vol. 13, no. 3, pp. 777–782, 1998.
[9] H. Muto, *et al.*, "Frequency spectrum due to standing waves excited by partial discharges in a GIS," in *10th International Symposium on High Voltage Engineering*, vol. 4, 1997, pp. 179–182.
[10] M. Lauersdolf, *et al.*, "Detection and suppression of Corona discharges during PD-measurement by means of RI-reception," in *IEEE International Symposium on Electrical lnsulation*, 1994, pp. 310–313.
[11] B. F. Hampton, *et al.*, "Diagnostic measurements at ultra high frequency in GIS," in *CIGRE 1990 Session*, 1990, 15/33-01.
[12] K. Masaki, *et al.*, "On-site measurement for the development of on-line partial discharge monitoring system in GIS," *IEEE Trans. Power Delivery*, vol. 9, no. 2, pp. 805–810, 1994.
[13] G. Wanninger, "Antennas as coupling devices for UHF diagnostics in GIS," in *9th International Symposium on High Voltage Engineering*, 1995, no. 5625.
[14] H. Okubo, *et al.*, "Partial discharge measurement in long distance SF_6 gas insulated transmission line (GIL)," *IEEE Trans. Power Delivery*, vol. 13, no. 3, pp. 683–690, 1998.
[15] M. Hikita, *et al.*, "Electromagnetic noise spectrum caused by partial discharge in air at high voltage substations," *IEEE Trans. Power Delivery*, vol. 13, no. 2, pp. 434–439, 1998.
[16] H. Okubo, *et al.*, "Electromagnetic spectrum radiated from gas discharges and its relation to partial-discharge characteristics," *European Trans. Electrical Power*, vol. 7, no. 1, pp. 57–63, 1997.

Toshihiro Hoshino was born on October 30, 1971. He received the M.S. degree in 1997 in electrical engineering from Nagoya University. Presently, he is a student in the Doctor's program of the Department of Electrical Engineering, Nagoya University. He is a student member of IEE of Japan.

Katsumi Kato was born on May 20, 1969. He received the Ph.D. in 1997 in electrical engineering from Nagoya University. Since 1997, he has been the faculty of Nagoya University. Presently, he is an Assistant Professor of Nagoya University at the Department of Electrical Engineering. He is a member of IEE of Japan.

Naoki Hayakawa was born on September 9, 1962. He received the Ph.D. degree in 1991 in electrical engineering from Nagoya University. Since 1990, he has been the faculty of Nagoya University. Presently, he is an Associate Professor of Nagoya University at the Department of Electrical Engineering. He is a Member of IEEE and IEE of Japan.

Hitoshi Okubo was born on October 29, 1948. He received the Ph.D. degree in 1984 in electrical engineering from Nagoya University. He joined Toshiba Corporation/Japan in 1973 and was a manager of high-voltage laboratory of Toshiba. From 1976 to 1978, he was at the RWTH Aachen/Germany and the TU Munich/Germany. Since 1989, he was an Associate Professor and presently he is a Professor of Nagoya University at the Department of Electrical Engineering. He is a Member of IEEE, IEE of Japan and VDE.